Ecotoxicology and Environmental Safety 228 (2021) 113006

Contents lists available at ScienceDirect

Ecotoxicology and Environmental Safety

journal homepage: www.elsevier.com/locate/ecoenv

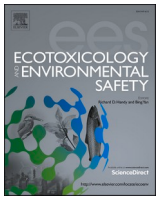

Preventive effects of *Lactobacillus johnsonii* on the renal injury of mice induced by high fluoride exposure: Insights from colonic microbiota and co-occurrence network analysis

Jinge Xin [a,1], Ning Sun [b,1], Hesong Wang [a,f,1], Hailin Ma [c,d,1], Bangyuan Wu [e], Lianxin Li [b], Yanyan Wang [b], Haonan Huang [b], Dong Zeng [b], Xiuquan Bai [f], Ali Chen [g], Shenhai Gong [h], Xueqin Ni [b,*], Yang Bai [a,**]

[a] *Guangdong Provincial Key Laboratory of Gastroenterology, Department of Gastroenterology, Institute of Gastroenterology of Guangdong Province, Nanfang Hospital, Southern Medical University, Guangzhou, China*
[b] *Animal Microecology Institute, College of Veterinary Medicine, Sichuan Agricultural University, Chengdu, Sichuan, China*
[c] *Plateau Brain Science Research Center, Tibet University, Lhasa 850012, China*
[d] *Plateau Brain Science Research Center, South China Normal University, Guangzhou 510631, China*
[e] *College of Life Sciences, China West Normal University , Nanchong , Sichuan, China*
[f] *Guangzhou Beneco biotechnology Co. Ltd., Guangzhou, China*
[g] *School of Chemistry and Chemical Engineering, Guangdong Pharmaceutical University, Guangzhou 510006, China*
[h] *School of Traditional Chinese Medicine, Southern Medical University, Guangzhou, China*

ARTICLE INFO

Keywords:
16S rRNA sequencing
Fluoride-induced damages
Gut microbota
Probiotics
Renal dysfunction

ABSTRACT

Fluoride (F) exposure was widely reported to be associated with renal diseases. Since absorbed F enters the organism from drinking water mostly through the gastrointestinal tract, investigating changes of gut microbes may have profound implications for the prevention of chronic F exposure because increasing evidence supported the existence of the gut-kidney axis. In the present study, we aimed to explore the potential positive effects of probiotics on high F exposure-induced renal lesions and dysfunction in mice by the modulation of the colonic microbiota. Mice were fed with normal (Ctrl group) or sodium-fluoride (F and Prob groups; 100 mg/L sodium fluoride (NaF)) drinking water with or without *Lactobaillus johnsonii* BS15, a probiotic strain proven to be preventive for F exposure. Mice fed with sodium-fluoride drinking water alone exhibited renal tissue damages, decreased the renal antioxidant capability and dysfunction. In contrast, *L. johnsonii* BS15 reversed these F-induced renal changes. 16S rRNA gene sequencing shows that *L. johnsonii* BS15 alleviated the increased community diversity (Shannon diversity) and richness index (number of observed features) as well as the distured structure of colon microbiota in F-exposed mice. A total of 13 OTUs with increased relative abundance were identified as the keystone OTUs in F-exposed mice based on the analysis of degree of co-occurrence and abundance of OTUs. Moreover, Spearman's rank correlation shows that the 13 keystone OTUs had negative effect on renal health and intestinal integrity. *L. johnsonii* BS15 reversed four of keystone OTUs (OTU 5, OTU 794, OTU 1035, and OTU 868) changes which might be related to the underlying protected mechanism of *L. johnsonii* BS15 against F-induced renal damages.

1. Introduction

Fluoride (F) is an essential chemical of social production (such as agriculture, food processing and industrial engineering) and maintains the organisms' health. Despite these benefits, there is a growing awareness of the adverse body impacts arising from excessive F intake over a prolonged period. These included increased skeletal and dental fluorosis as a result of long-term excessive F exposure. Obvious damages

* Correspondence to: 211 Huimin Road, Chengdu 610400, Sichuan, China.
** Correspondence to: 1838 Guangzhou Avenue, Guangzhou 510000, Guangdong, China.
E-mail addresses: xueqinni@foxmail.com (X. Ni), 13925001665@163.com (Y. Bai).
[1] These authors are equal contributors.

https://doi.org/10.1016/j.ecoenv.2021.113006
Received 8 August 2021; Received in revised form 15 November 2021; Accepted 16 November 2021
Available online 23 November 2021

of kidney, liver, spleen, blood, gastrointestinal tract and nervous system were also observed in previous studies (Petersson et al., 2011). Many countries have reported that excessive F exposure is mainly due to the high fluoride groundwater linked to geological factors. Moreover, the number of people exposed to high fluoride is approximately 200 million in 25 countries around the world, especially in Asia, Europe, Africa, North and South America (Ayoob and Gupta, 2006).

To date, many studies have demonstrated that high F exposure over a long period affects the kidney by histopathological changes and oxidative stress. Basha and Rao et al. (2014) found that renal toxicity of fluoride is time-dependent. Furthermore, epidemiological investigation from the United States suggested that complex renal damages in the adolescent population are associated with F exposure (Malin et al., 2019). However, the exact mechanism underlying F-induced renal damages remains unclear, which makes it difficult to find a preventive method against high F exposure. Nowadays, a lot of clinical trials and experimental results in nephropathic diseases have revealed that the administration of probiotics could attenuate colonic epithelial tight junction disruption and reduce the levels of uremic toxins and inflammatory mediators (Vaziri et al., 2014). In our previous study, we also found that excessive F intake affected the normal intestinal microbial communities, resulting in the damages of mucosal barrier function and intestinal villi development (Sun et al., 2020). Evidence is accumulating to consider gut microbiome as an essential role in the gut-kidney axis. The regulation of intestinal flora may be an effective way to alleviate kidney deleterious induced by high fluoride exposure by promoting or maintaining intestinal health. Nevertheless, more evidence based on animal experiments should be provided to demonstrate the relationship between the variations of intestinal tract and renal tissue under different conditions (Yang et al., 2018). The beneficial effects of gut microbiota in the colon against high F intake in drinking water remain unexplored.

Previous researches demonstrated that the abundance of beneficial bacteria was decreased in nephropathic disease, which makes it possible to reverse the renal lesions by applying probiotics. *Lactobacillus* is one of the most common beneficial bacteria applied in renal diseases. Oral administration of an antibiotic-resistant *Lactobacillus* preparation (known as Lebenin) could restore the composition of intestinal microbial population to normal in patients with uremia and inhibit the accumulation of uremia toxins in the blood (Hida et al., 1996). Such influences of lactic acid bacteria could be the result of its impacts on the immune status and permeability of the gut epithelium. *Lactobacillus johnsonii* BS15, a potential probiotic strain, has been reported its beneficial effects in preventing obesity-induced nonalcoholic fatty liver disease in mice (Xin et al., 2014). Our previous study reported *L. johnsonii* BS15 could effectively improve the dominant species abundance and gut development of small intestine under high F environment, resulting in exerting beneficial effects on the gut-brain axis (Sun et al., 2020; Xin et al., 2021), but underlying mechanism still needs in-depth study. In addition, the effects of *L. johnsonii* BS15 on preventing renal dysfunction and the underlying mechanism are also necessary to be demonstrated.

We thus investigated the influences of high F exposure and probiotic supplementation on colonic bacterial communities in mice using amplicon sequencing, tissue physiology and biochemistry analysis. From the perspective of physiological and pathological metabolic processes, we evaluated the renal injury through excessive F exposure by observing histopathological lesions, functional changes and oxidative damage. In addition, it is unclear that whether or not community composition and diversity in colonic microbiome under high F environment reconstruct corresponding species pattern. Therefore, an animal experiment combining these two aspects under the same experimental conditions allows to investigate the effects of excessive F-induced damages and probiotic treatment on microbial communities of colon and pathological changes of renal tissue. Using 16 S rDNA sequencing technique, we aimed to unravel how colonic microbial communities respond to excessive F exposure and probiotic supplementation. We specifically asked: (1) Whether or not supplementation with *L. johnsonii* BS15 could play an important role in preventing renal lesions induced by high F exposure over a long period? (2) Do colonic microbes communities differ in their responses to high F exposure and *L. johnsonii* BS15 supplementation? (3) Which microbes could be considered as the indicator taxa for different conditions (high F exposure vs. *L. johnsonii* BS15)? (4) How do high F exposure and *L. johnsonii* BS15 impact co-occurrence patterns of colon-associated microbes?

2. Material and methods

2.1. Cultrue and treatment with BS15

The heterotrophic bacteria strain, *Lactobacillus johnsonii* BS15, was cultured in de Man, Rogosa and Sharpe (MRS) broth at 37 ℃. Plate count method was used to count the bacteria cells. Briefly, bacteria solution was diluted with PBS by a gradient of 10 times. The dilution gradient of 10^{-5}, 10^{-6}, and 10^{-7} were choosed and each gradient was drawn 10 μL to drop on the MRS agar medium, repeated three times. Then the MRS agar medium was cultured 36 h at 37 ℃. The appropriate gradient (easy for counting the bacteria) was selected for bacteria counting. Next, a centrifuge (3000×rpm, 4 ℃, 15 min) and wash separated the cells from the cultures and resuspended in phosphate buffered saline (PBS) (PH 7.0) for experimental use. Concentration of suspension were 1×10^9 CFU BS15/mL (daily consumption dose: 0.2 mL/mice) (Xin et al., 2014).

2.2. Animals treatment, study design and sampling

Three-week-old male specific-pathogen-free ICR (Institute for Cancer Research) mice (Chengdu Dashuo Biological Institute, Chengdu, China) with similar body weights were bred at the Animal Microecology Institute in Sichuan Agricultural University in Sichuan, China. A total of 30 SPF mice were randomly allocated to three groups (Ctrl, F and Prob groups) to characterize the change in tissues and local microbial community by different treatments. These mice were fed standard laboratory chow (Chengdu Dashuo Biological Institute) and allowed free access to water for 1 week to acclimatize new environment, in a controlled temperature (22 ± 2 ℃) room with a 12-h light-dark cycle. After the adaptation period, mice were administered with either PBS (Ctrl and F groups) or BS15 (Prob group) by gavage throughout the whole experimental period (98d). In addition, mice in F and Prob group were fed fluoride drinking water (100 mg NaF /L) during the high F exposure period (29–98d). As a result, a total of three treatments were included in this experiment: no treatment (Ctrl) mice, F alone treatment (F) mice, F and probiotic co-treatments (Prob) mice. All animal experiments were performed according to the guidelines for the care and use of laboratory animals approved by the institutional ethical committee (approval number: SYXKchuan2019–187).

Urine of these mice were collected before sampling. At 105th day of the experiment, blood were sampled from the mice orbit before they were sacrificed. Serum was separated by incubation at 4 ℃ over night, followed by centrifugation at 3000 ×rpm for 20 min at 4 ℃ and stored at − 80 ℃. Subsequently, 10 mice per groups were sacrificed by cervical dislocation in accordance with institutional animal care guidelines. kidney and partial distal colon were collected and rinsed with ice-cold saline and immediately stored at − 80 ℃. Part of kidney and colonic tissues were fixed in 4% paraformaldehyde solution for histopathologic examination, villus morphology measurement and goblet cells observation.

2.3. Histological analysis

Kidney and colonic tissues were dehydrated with increasing concentrations of absolute ethanol, cleared with xylene, and saturated with and embedded in paraffin.

Tissue samples were serial sectioned at 5 μm thickness, srained with hematoxylin and eosin (H.E.), and observed by light microscopy

(Olympus, Tokyo, Japan).

2.4. Biochemical test

The activity of N-acetyl-b-D-glucosaminidase (NAG) in the urine samples of mice were measured using a commercial kit by biochemical methods provided by Nanjing Jiancheng Bioengineering Institute (A301; Nanjing, Jiangsu, China). The contents of Blood urea nitrogen (BUN), Creatinine (Cr) and Uric acid (UA) in serum were quantified by biochemical methods following the instructions of the commercial kits (BUN, C013–2; Cr, C011–2; UA, C011–2; Nanjing, Jiangsu China).

Right kidney were grinded into 10% homogenate with PBS (0.01 mol/L) by glass homogenizer, and supernatant was obtained by centrifugation at 4 ℃ and 12,000g for 5 min. Then the liquid supernatant was collected for the determination of total protein, Na+ /K+ -ATPase, acid phosphatase (ACP), Lactate dehydrogenase (LDH), anti-superoxide anion (ASA), anti-hydroxyl radical (AHR), superoxide dismutase (SOD), catalase (CAT), glutathione peroxidase (GSH-Px) activities and glutathione (GSH), malondialdehyde (MDA), and Protein carbonyls (PC) contents using a biochemical kits provided by Nanjing Jiancheng Bioengineering Institute (total protein, A405–2; Na^+/K^+-ATPase, A016–1; ACP, A060–2; LDH, A020–2; ASA, A052; AHR, A018; SOD, A001–1; CAT, A007–1; GSH-Px, A005; GSH, A006–2; MDA, A003–1; PC, A087; Nanjing, Jiangsu, China).

2.5. Real-time quantitaive PCR (RT-qPCR) test of mRNA expression levels

Total kidney and colon RNA were isolated by using E.Z.N.A.® Total RNA Kit (OMEGA BioTek, Doraville, GA, USA) according to the manufacturer's guidelines. The quantity and quality of isolated RNA were assessed quantitatively and qualitatively from agarose gel electrophoresis as well as absorbance ratios of 260 nm and 280 nm. In accordance with manufacturer's instruction of the Prime Script TM RT reagent kit with gDNA Eraser (Thermo Scientific, Waltham, Massachusetts, USA), 1 μg isolated RNA synthesized the first-strand complementary DNA (cDNA). Subsequently, the cDNA products were frozen at − 20 ℃ for further research of gene expression. RT-qPCR test was performed by using a LightCycle®96 Real-Time system (Boehringer Mannheim GmbH, Germany) with SYBR Green Supermix (Bio-Rad, Hercules, CA, USA). The reaction mixture included cDNA products (1 μL), forward and reverse primers (2 μL), SYBR Green Supermix (5 μL) and sterile deionized water (2 μL). And the RNA protocol was implemented predenaturation for 5 min at 95 ℃, followed by 40 cycles of 10 s denaturation at 95 ℃ and 30 s annealing at optimum temperature. The final melting curve analysis was monitored to the purity of the PCR products. primer sequences and optimum temperature of each target gene were consisted with Xin et al. (2021). And the relative gene expression levels was shown as fold changes after normalization to the β-actin, and the data were calculated by using Microsoft Excel Software with $2^{-\triangle\triangle Cq}$ relative abundance method. The mRNA levels of Claudin-1, Occludin, and ZO-1 in the colon were detected from each group.

2.6. Statistical analysis of biochemical and RT-qPCR tests

All results were reported by mean ± standard deviation. Normality was evaluated using the Shapiro -Wilk normality test. If data were not normally distributed they were log transformed for analysis. Data that remained not normally distributed were analyzed by Kruskal-Wallis test followed by Wilcoxon test. All data were assessed by one-way analysis of variance (ANOVA) followed bypost hoc least significant difference (LSD). Differences of $p < 0.05$ were considered as statistically significant. Data were analyzed with IBM SPSS Statistics 25.

2.7. 16S rRNA sequencing data analysis

2.7.1. DNA extraction, 16S rRNA gene-targeted amplicon sequencing and DNA library preparation, and sequencing

DNA was extracted from colon content using the E.Z.N.A. Stool DNA isolation in accordance with the manufacturer's instruction. The concentration and purity of DNA were monitored on 1% (w/v) agarose gel electrophoresis. PCR amplification of the 16S rRNA gene was performed used specific primer (515F-806R) with the barcode. All PCR reactions were carried out in 30 μL reactions with 0.2 μM of forward and reverse primers, 15 μL of Phusion® High-fidelity PCR Master Mix (New England Biolabs), and about 10 ng template DNA. Mixture PCR products was purified with GeneJET™Gel Extraction Kit (Thermo Scientific). Subsequently, the amplified and purified DNA of each sample were enzymatically sheared, end-repaired and adapter ligated using Ion Plus Fragment Library Kit 48 rxns (Thermo Scientific) following manufacturer's recommendations. Lastly, purified PCR product were sequenced using the IonS5™XL platform and 400 bp/600 bp single-end reads were generated by the Novogene company.

Based on the unique barcode, single-end reads was assigned to different samples, and the barcode and primer sequence were truncated by cutting. Cutadapt then was used to quality filtering on the raw reads under specific filtering conditions. The reads were compared with the reference database (SILVA database, https://www.arb-silva.de/) using UCHIME algorithm (UCHIME Algorithm, http://www.drive5.com/usearch/manual/uchime_algo.html) to detect chimera sequences, and then the chimera sequences were removed to obtain the Clean Reads. Sequences anlysis about Operation Taxonomic units were performed by Uparse software (Uparse v7.0.1001, http://drive5.com/uparse/), with a clustering threshold of 97%. For each representative sequence, taxonomy was assigned using the Mothur algorithm (v1.35.1, http://www.mothur.org/) against the Silva Database (SILVA database, http://www.arb-silva.de/). In order to study phylogenetic relationship of different OTUs, and the difference of the dominant species in different samples (groups), multiple sequence alignment were conducted using the MUSCLE software (v3.8.31, http://www.drive5.com/muscle/). Following analyses of colonic microbes were performed in R v4.0.2.

2.7.2. Alpha diversity

Rarefaction analysis was conducted in QIIME (Version1.9.1) (Caporaso et al., 2021) and visualized with R software (Version 4.0.2). According to the sample with the least sequences, a standard of sequence number (44171, bacteria) per sample were used to normalized the OTUs abundance information, and alpha diversity was performed basing on this output normalized data. Complexity of species diversity (α-diversity) were evaluated for each sample based on observed OTUs richness and shannon diversity. We calculated the difference to different treatments on richness and diversity using Kruskal-Wallis test and pairwise Wilcoxon test from R software.

2.7.3. Beta diversity

We conducted exploratory analysis of beta diversity (β-diversity) on the bacterial communities of colon comparing different treatments. For the exploratory analysis, we used the following reads count threshold to the filtered absolute OTU table: we selected OTUs with at least two reads (avoiding single-count OTUs) in at least ten samples (the number of replicates per group). We considered OTUs remaining after this thresholding condition to be colonic communities of each treatment. Then, we normalized the filtered absolute OTU table for microbial communities using the "Relative log expression (RLE)" method with the BioConductor package *DESeq2*. Subsquently, we quantified the major variance components and visualized from multidimensional data by unconstrained principle coordinates analysis (PCoA) on Bray-Curtis dissimilarities in colonic bacterial communities. Ordination analyses were conducted by the R package *phyloseq*. For the in-depth assessment of all treatments, We conducted statistical analysis of microbial diversity

based on the methods outlined by Hartman (Hartman et al., 2018). In short, This included a constrained analysis of principal coordinates (CAP) verifying the effects of high F exposure and *L. johnsonii* BS15 treatment, statistical testing of the different treatment hypothesis, and identification of the species (OTUs) responsible for the effects of visualization. Above all, ordination analyses were conducted using the package *phyloseq* of R. Then statistical significance of the CAP was analyzed by the *permutest* method in the R package *vegan* with 10^4 permutations. And we tested for high F exposure and probiotic effects on microbial community using permutational analysis of multivariate dispersions (BETADISP) and permutational analysis of variance (PERMANOVA) by the methods of *betadisp* and *adonis*, respectively, in the R package vegan with permutations. Lastly, we assessed the pairwise differences between the three groups with the *pairwise.perm.manova* function from the *RVAideMemoire* package.

2.7.4. Species clustering analysis

We performed species clustering analysis of relative abundance on the bacterial communities comparing each sample or group. Subsequently, we tested for the significant alterations of microbial taxa, including phylum and genus, between each treatments using pairwise wilcoxon test. Linear discriminant analysis effect size (LEfSe) was applied to identify biomarker(s) differentially represented in the colonic bacterial community by different groups. There are linear discriminate analysis with the standard test for statistical significance, including Kruskal-Wallis test and pairwise Wilcoxon test. For testing the most differentially abundant taxa between each treatments, LEfSe analysis was processed under the following conditions: microbial taxa whose p value (factorial Kruskal-Wallis test) and the threshold for discriminative features (logarithmic LDA score) were calculated among the each group at $P < 0.05$ and LDA Socre > 4.0, respectively. And additionally, we constructed the correlation network by Spearman rank algorithm in each group as implemented in the package *igraph* (Csardi G). In these networks, the nodes represented the genus of microbial taxa, where the edges corresponded to a positive (red) or negative (blue) correlation and significant value ($P < 0.05$) between the nodes. Moreover, the size of nodes and width of edges represented taxa abundance and correlation intension of microbial community in each group separately.

2.7.5. Identification of high F exposure sensitive OTUs (fsOTUs), high F exposure and L. johnsonii BS15 co-sensitive OTUs (flsOTUs)

Two complementary approaches were employed to identify the species (OTUs) responsible for the observed effects. Firstly, indicator species analysis was applied to calculate the coefficient r (point-biserial correlation coefficient) of an OTU's positive related to one or more of different treatments. And this analysis was performed with 10^4 permutations and filtrated significant at $P < 0.05$. Then, we identified the differential OTUs between each group using Wald Test (WT) analysis in the *DESeq2* package. OTUs whose abundances were considered as differing between each group at a log2 Fold Change (log2FC) of $|\log2FC > 1$, and a false discovery rate (FDR) corrected p value of $q < 0.05$ were selected to be different treatment responsive. Lastly, we defined OTUs that were identified by the complementary results of indicator species analysis and WT analysis as three groups of species responding differently. These included: the control specific OTUs (csOTUs), high F exposure sensitive OTUs (fsOTUs), as well as high F exposure and *L. johnsonii* BS15 co-sensitive OTUs (flsOTUs).

2.7.6. Bipartite network and co-occurrence network

Significant difference ($P < 0.05$) OTUs of which the differences were calculated using the indicator species analysis between one or more of the different treatments were visualized by bipartite network. Bipartite network were constructed by the Fruchterman-Reingold layout with 10^4 permutations using the R package *igraph*. Then, we also visualized the results based on WT analysis to observe the differential OTU between each groups.

For the in-depth comparison and analysis of bacterial communities, we constructed co-occurrence network to visualize correlations in all species. For this, we utilized the RLE normalized OTU counts and calculated Spearman rank correlations between OTUs, and visualized the high-positive, significant correlations ($\rho > 0.6$ and $P < 0.01$). And additionally, we calculated the topological network propertoes using the R package *igraph*. These included: (1) number of nodes of network; (2) number of edges (connections) between nodes; and (3) degrees of co-occurrence of a node. To explore bacterial community structure within the colonic microbial network, we identified network modules using the *greedy optimization of modularity* algorithm in the R package *igraph*. These modules are a collection of nodes with a higher density of edges in network within groups than between them. Similarly, co-occurrence network was constructed by the *Kamada-Kawai layout* with 10^4 permutations in the *igraph* package of R software.

Lastly, the microbes that constantly co-occur with other groups are considered to be important ecological significance and may play a key role in the microbial community in the co-occurrence network. For this, keystone OTUs were defined as the top 3% of node degree values and were confirmed in the co-occurrence network. In order to further observe the relationships between keystone OTUs and renal functions as well as colon permeability, We then constructed the visualized heatmap using Spearman rank correlations between them as implemented in packages *psych*. And all of the above microbial group analysis was implemented in R software.

3. Results

3.1. Effects of high F exposure and L. johnsonii BS15 on histopathological changes in the kidney tissue

As shown in Fig. 1A, no obvious changes were observed in the renal tissue of Ctrl group. Fig. 1B showed that the epithelial cells of the renal tubules were swollen and there was severe granular as well as vaculolar degeneration in F group. In addition, the telangiectasia between glomeruli and renal tubules was hyperemia in the F group. However, change in the Prob group (Fig. 1C) were similar to those in the Ctrl group. It was only slight dilatation and congestion of capillaries between glomeruli and renal tubules.

3.2. Changes of chemical parameters in the serum, urine and kidney tissue

As shown in Fig. 2, although BUN content showed no significant difference ($p > 0.05$) (Fig. 1B), all other determined parameters changed significantly ($P < 0.05$ or 0.01) among three experimental groups. Fig. 1A shows that the NAG activity in the urine was significantly increased ($P < 0.01$) in F group compared with that in Ctrl and Prob groups, whereas this parameter in Prob group significantly increased ($P < 0.01$) compared with Ctrl group.In addition, compared with the Ctrl and Prob groups, the serum Cr and UA contents were markedly increased ($P < 0.01$) in the F group, whereas the serum Cr content was significantly decreased ($P < 0.05$) in the Prob group in comparison with those in the Ctrl group (Figs. 1C and 1D). Significant changes ($P < 0.01$) of Na+ /K+ -ATPase activity between groups were detected in Fig. 1E. Moreover, results in Figs. 1F and 1G showed significantly higher ($P < 0.05$ or 0.01) LDH activity and lower ($P < 0.05$ or $P < 0.01$) ACP activity in F group than those in the Ctrl and P group, but no significant difference ($P > 0.05$) was observed between Ctrl group and Prob group.

3.3. Peroxidation damage and antioxidant capacity in the kidney tissue

As shown in Fig. 3 A and 3B, the MDA and PC contents in the F group were significantly higher ($P < 0.01$) than those in the Ctrl and Prob groups. Similarly, significant changes ($P < 0.01$) were detected in those peroxidation damage related parameters between Ctrl group and F

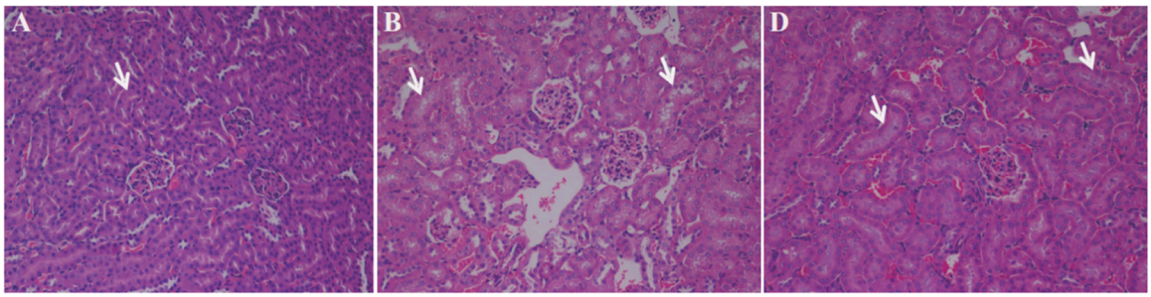

Fig. 1. Histopathological changes in the kidney tissue of mice. Histological observation of ileum under original magnification (100 ×). (A)Kideny tissue in Ctrl group; (B) Kideny tissue in F group; (C) Kideny tissue in Prob group. The swell, severe granular degeneration as well as vacuolization of the epithelial cells of fluoride-exposure mice was indicated by white arrows.

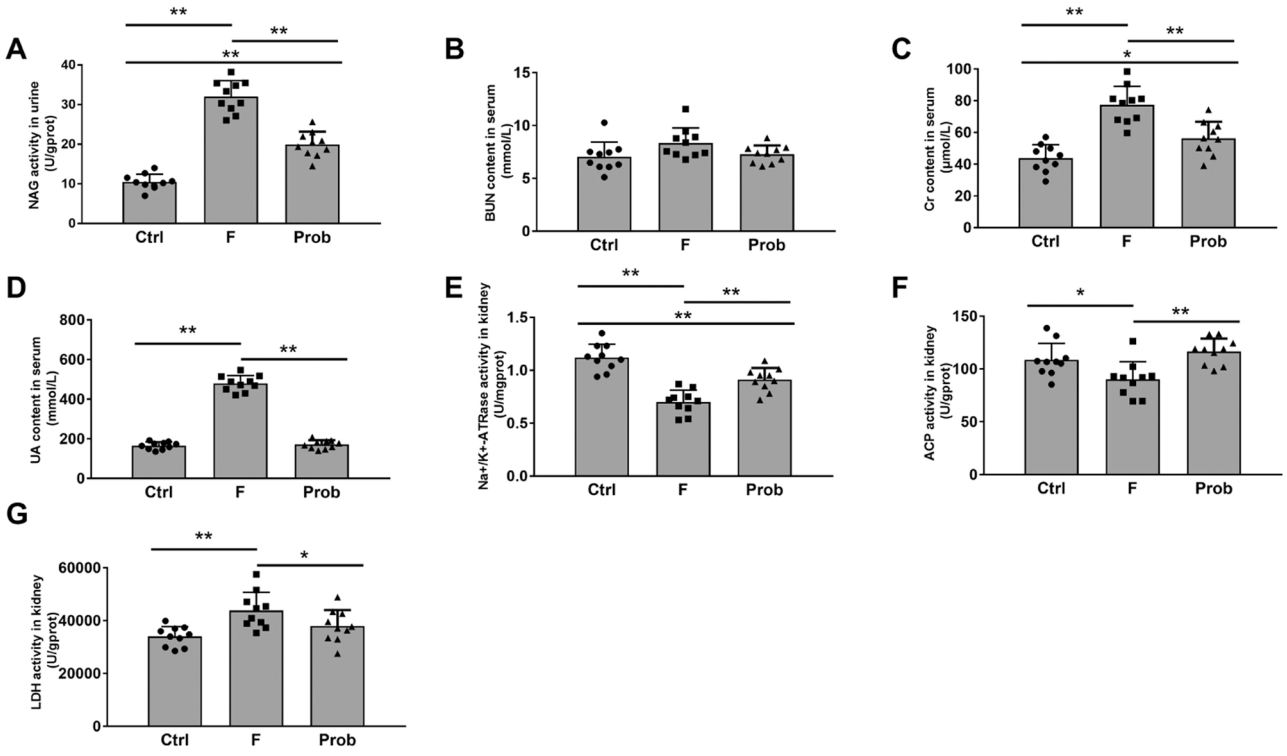

Fig. 2. Changes of chemical parameters in the serum, urine and kidney tissue. (A) NAG activity in urine ($F_{2,\ 27}$ =115.92, $P < 0.001$). (B) BUN content in serum ($F_{2,\ 27}$ =3.022, $P = 0.065$). (C) Cr content in serum ($F_{2,\ 27}$ =26.98, $P < 0.001$). (D) UA content in serum ($F_{2,\ 27}$ =400.13, $P < 0.001$). (E) Na^{+}/K^{+}-ATPase activity in kidney tissue ($F_{2,\ 27}$ =32.90, $P < 0.001$). (F) ACP activity in kidney tissue ($F_{2,\ 27}$ =8.08, $P = 0.002$). (G) LDH activity in kidney tissue ($F_{2,\ 27}$ =7.40, $P = 0.003$). Data are presented with the mean ± standard deviation (n = 10). Significance between groups was indicated with asterisk(* $p < 0.05$, ** $p < 0.01$). NAG, N-acetyl-b-D-glucosaminidase; BUN, blood urea nitrogen; Cr, creatinine; UA, uric acid; Na+ /K+ -ATPase, sodium-potassium adenosine triphosphatase; ACP, acid phosphatase; LDH, lactate dehydrogenase.

group. In addition, there were significantly reductions ($P < 0.01$) in the ASA and AHR activities of the kidney tissue in the F group compared with the Ctrl group, but those indexes show no signicant difference ($P > 0.05$) in the Prob group compared with the other two groups (Fig. 3 C and 3D). According to results shown in Fig. 3E-3 H, the activities and contents of antioxidases and antioxidant substances (SOD, CAT, GSH-Px and GSH) in the kidney were significantly lower ($P < 0.01$ or $P < 0.05$) in the F group compared with the other two groups except for CAT activity which shows no significant difference between the F and Prob group ($P > 0.05$). Meanwhile, significant changes ($P < 0.01$ or $P < 0.05$) of SOD, CAT and GSH-Px activities as well as GSH content were observed between Ctrl and Prob groups.

3.4. *Effect of L. johnsonii BS15 on Claudin-1, Occludin and ZO-1 mRNA expression levels in the colon*

In the results of intestinal permeability of colon tissue (Fig. S1A-B), significantly lower ($P < 0.05$ or $P < 0.01$) mRNA levels of Occludin and ZO-1 were found in F group compared with those in Ctrl and Prob groups (Fig. S1B and S1C), but there was a slight reduction ($P > 0.05$) in the mRNA level of Claudin-1 (Fig. S1A). Although significant difference ($P < 0.01$) was observed in the mRNA level of Occludin between Ctrl and Prob groups (Fig. S1B), the mRNA level of Claudin-1 showed significant higher ($P < 0.01$) than that in Ctrl and F group (Fig. S1A).

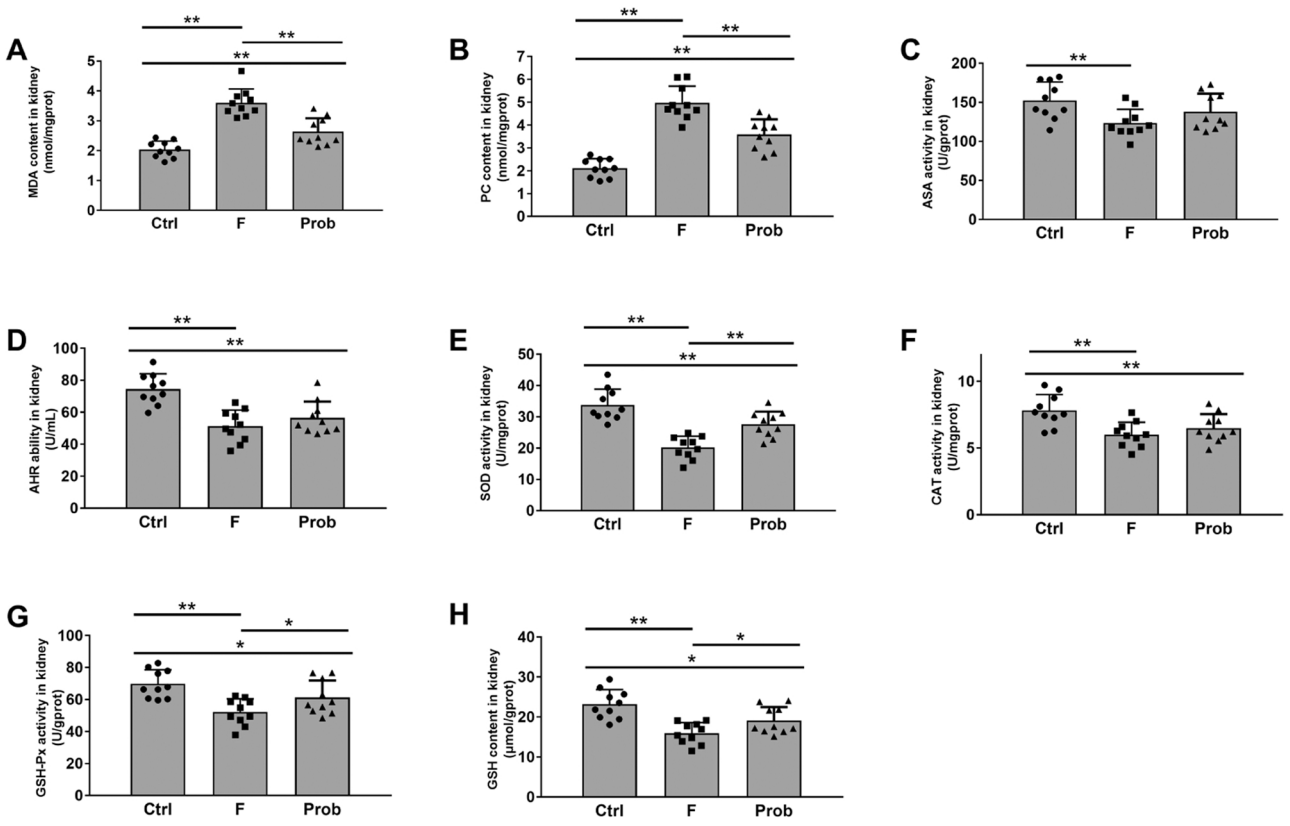

Fig. 3. Change of peroxidation damage and antioxidant capacity in the kidney. (A) MDA content. ($F_{2,\ 27}$ =37.37, $P < 0.001$). (B) PC content ($F_{2,\ 27}$ =53.38, $P < 0.001$). (C) ASA activity ($F_{2,\ 27} = 4.52$, $P = 0.020$). (D) AHR ability ($F_{2,\ 27}$ =14.83, $P < 0.001$). (E) SOD activity ($F_{2,\ 27}$ =25.38, $P < 0.001$). (F) CAT activity ($F_{2,\ 27}$ =7.85, $P = 0.002$). (G) GSH-Px activity ($F_{2,\ 27}$ =9.06, $P = 0.001$). (H) GSH content ($F_{2,\ 27}$ =12.33, $P < 0.001$). Data are presented with the mean ± standard deviation (n = 10). Significance between groups was indicated with asterisk(* $p < 0.05$, ** $p < 0.01$). MDA, malondialdehyde. PC: protein carbonyls. ASA: anti-superoxide anion; AHR: anti-hydroxyl radical. SOD, superoxide dismutase. CAT, catalase. GSH-Px, glutathione peroxidase. GSH, glutathione.

3.5. L. johnsonii BS15 alleviated the fluoride-induced disturbation of colon microbial diversity

Bacteria community in colonic luminal contents was measured using Illumina Miseq sequencing to investigate the effects of high F exposure and *L. johnsonii* BS15. A total of 1028 OTUs, with an average of 448 OTUs per sample, were identified from 2,327,431 quality-filtered sequences in the all samples. To evaluate the within-community (α-diversity) in colonic microbiome, we rarified the communities to the least sequences (44171 reads) per sample, which represent most of the observed species richness were captured at microbiota community (Fig. S1D). Observed OTU richness and shannon diversity was highest in F samples with significant effect ($P < 0.05$) for bacterial communities than that in Ctrl sample, whereas no significant difference was observed between the Ctrl and Prob group ($P > 0.05$; Fig. S1E and S1F).

Similarly, the colon presents different microbial community composition among samples. We tested the patterns of separation between microbial communities (β-diversity) by unconstrained principal coordinate analysis (PCoA) on Bray-Curtis dissimilarities (Fig. S1G). Microbial communities of Ctrl and F samples clearly separated along the first principal coordinate (27.8%). Prob samples showed a significantly separation with the other two groups. Compared with the F group, Prob samples seems to be nearer to the Ctrl group (Fig. S1G). The separation among the three groups were also demonstrated by canonical analysis of principal coordinates (CAP) (Fig. S1H) and permutational multivariate analysis of variance (PERMANOVA) (Table S1). The result of PCoA analysis corroborates that high F exposure comprises the largest source of variation within the colonic microbiome when using a Bray-Curtis distance metric. Since β-diversity can be influenced by differences in true biological impact, group dispersion (variance), or both, we calculated and identified the differences in dispersion for colonic microbiota using BETADISP (Table S1). The lack of significance in this dispersion results revealed difference among three groups were influenced primarily by true biological impacts and not an artifact of impact of within-group dispersion. Therefore, F-driven alone difference were seen in the F and Ctrl bacterial communities. Similarly, probiotics also appeared to be the new driving factor in colonic bacteria.

3.6. L. johnsonii BS15 inhibited the fluoride-induced changes of dominant bacteria taxa

Microbial taxa difference among Ctrl, F and Prob groups were evident in the taxonomic analysis of all sample types. We noted 16 bacteria phyla present in colonic samples, with Firmicutes, Bacteroidetes and Actinobacteria having the highest relative abundances (Fig. S1I). Other bacterial phyla were classified as low abundance levels (less than 1%), including Proteobacteria, Tenericutes and Melainabacteria. Firmicutes was the most prominent gut bacterial community in the Ctrl and prob group, accounting for an average of 80.3% and 68.7% sequence, respectively (Fig. S1I and S1K). The relative abundance of Firmicutes was significantly decreased in F group compared to the Ctrl group (wilcoxon test, $P < 0.01$; Fig. S2a), and the percentage of Firmicutes in the F group was 37.1%. However, adequate probiotic intake significantly alleviated the decrease in the proportion of Firmicutes (wilcoxon test, $P < 0.01$; Fig. S2A). Bacteroidetes represented the second dominant gut microbiome in the Ctrl and P group, accounting for an average of 12.9% and 25.9% sequences, respectively (Fig. S1I and S1K). The percentage of Bacteroidetes in the F group was 52.8%, demonstrating that the relative abundance of Bacteroidetes was significantly increased under the influence of F alone compared with control mice

(wilcoxon test, $P < 0.01$; Fig. S2B). At the genera level, the most prominent colonic microbiota community in the Ctrl and Prob groups was *Lactobacillus*, while it was *Bacteroides* in F group. The percentage of *Lactobacillu* was respectively,54.6%, 2.9% and 46.2% in the Ctrl, F and Prob groups. while *Bacteroides* was 2.1%, 19.9% and 11.5% respectively (Fig. S1J and S1K). The next dominant genus were composed of *Dubosiella*, *Helicobacter* and *unidentified Lachnospiraceae*, contributing 8.2%, 4.1% and 1.6% of the Ctrl group, 2.5%, 5.4% and 4.0% of the F group, and 2.9%, 2.0% and 3.0% group, respectively (Fig. S1J and S1K). As shown in Fig. S2, F group had significantly higher (wilcoxon test, $P < 0.01$ or $P < 0.05$) abundance of *Bacteroides*, *Alistipes*, *Alloprevotella, Erysipelatoclostridium*, *unidentified Ruminococcaceae*, . Moreover, the abundance of *Lactobacillus* was significantly (wilcoxon test, $P < 0.01$) reduced in F group compared with the Ctrl and Prob group. Differing greatly from the results in F group, supplementation with *L. johnsonii* BS15 after high F exposure has a significantly greater proportion of *Lactobacillus* (wilcoxon test, $P < 0.01$; Fig S2C).

Biomarkers in colonic microbiota between different groups were detected using the Linear discriminant analysis Effect Size (LefSe; Fig. 4). The histogram generated from the LEfSe analysis showed the most differentially abundant taxa enriched in colonic microbiota from three groups (Fig. 4A and 4B). Meanwhile, The cladogram indicated that a difference of microbial phylotypes was observed between different treatments (Fig. 4C and 4D). LefSe analysis might serve as an effective analysis that define biomarkers to differentiate between Ctrl, F and Prob populations. As shown in Fig. 4A and 4C, Firmicutes, *Bacilli,*

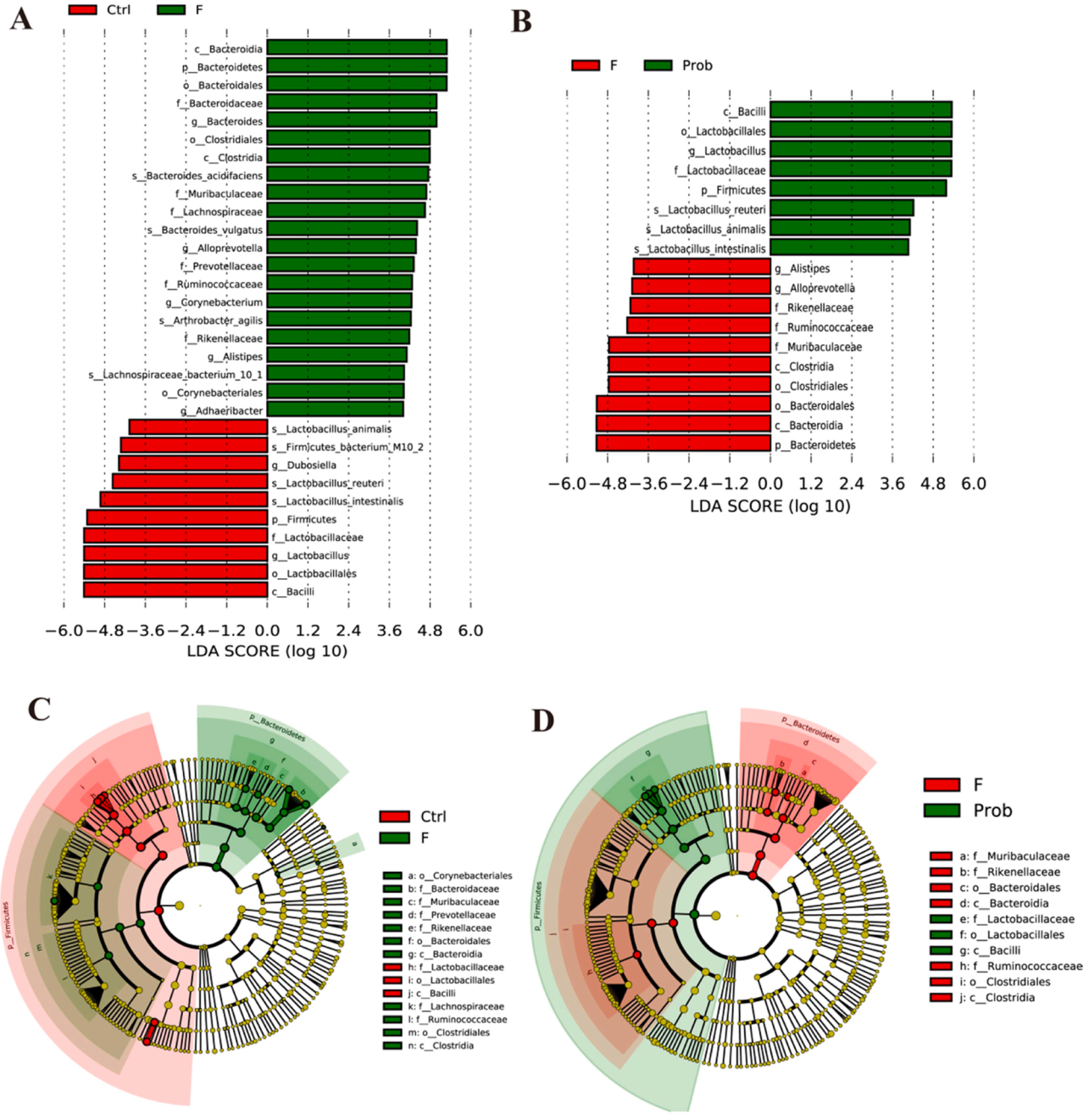

Fig. 4. Linear Discriminant Analysis Effect Size Analysis. Significantly discriminative taxa (Biomarkers) between the Ctrl and F groups of mice were displayed by LDA value distribution histogram (A) and cladogram (C). Significantly discriminative taxa (Biomarkers) between the F and Prob groups of mice were displayed by LDA value distribution histogram (B) and cladogram (D). Only taxa meeting the LDA significance thresholds (>4) are shown. Different coloured bars and regions represent different groups. From the interior to the exterior, each layer represents the phylum, class, order, family, and genus levels.

Lactobacillaceae, Lactobacillus, Carnobacterium, Lactobacillus intestinalis, Carnbacterium maltaromaticum, Lactobacillus reuteri, Firmicutes *bacterium M10 2 and Lactobacillus animalis* were more enriched in the Ctrl group (LDA score > 4.0), whereas Bacteroidetes, *Bacteroidia, Clostridia, Clostridiales, Bacteroidaceae, Muribaculaceae, Lachnospiraceae, Ruminococcaceae, Prevotellaceae, Rikenellaceae, Bacteroides, Alloprevotella, Alistipes, Bacteroides acidifaciens* and *Bacteroides vulgatus* were more abundant in the F group in the comparison between the Ctrl and F groups (LDA score > 4.0). In addition, we found that *Alistipes, Alloprevotella, Rikenellaceae, Ruminococcaceae, Muribaculaceae, Clostridia, Clostridiales, Bacteroidales, Bacteroidia* and Bacteroidetes were biomarkers in the F group (LDA score > 4.0, Figs. 4B and 4D). Additionally, *Bacilli, Lactobacillales, Lactobacillus, Lactobacillaceae, Firmcutes, Lactobacillus reuteri, Lactobacillus animalis* and *Lactobacillus intestinalis* were biomarkers in the Prob group (LDA score > 4.0; Figs. 4B and 4D).

Lastly, we showed that the differing treatment mode markedly altered microbial correlation patterns of genera levels in colon (Fig. S3; Table S2). Network connectivity (connections between nodes representing highly correlation, significant correlations between genus) was highest in the Prob group than the Ctrl and F bacteria networks. The bacterial network of F group comprised the fewest genus (node numbers) and was the least complex (identified by number of connections per genus).

In summary, although highly F-driven impacts were seen in the colonic bacterial community, the supplementation with *L. johnsonii* BS15 appeared to be the main mitigating factor in the variation of microbial taxa.

3.7. Identifying of Ctrl group specific OTUs (csOTUs), high F sensitive OTUs (fsOTUs), and high F and L. johnsonii BS15 co-sensitive OTUs (flsOTUs)

We performed indicator species analysis to select individual bacteria (OTUs) in colonic community whose abundances markedly altered in different treatments, and we visualized the analysis with a bipartite network (Fig. 5 A). The high number of colonic bacteria OTUs that were shared between F and Prob groups reflects the similar clustering of two sample types in the bacteria communities. Conversely, the little number or no number of bacteria OTUs were shared between Ctrl and F samples or Ctrl and Prob samples.

Since indicator OTUs were solely confirmed based on correlation, we further identified key species using Wald Test implemented in *DESeq2* (Fig. 5B). Significant enrichment or depletion of the filtered OTUs were identified between each treatments as determined by differential species analysis. As shown in Fig. 5B, each points in comparison between groups represents an individual OTU. The position along the x axis represents the abundance log2 Fold Change (log2FC), and the position along the y axis represents the $-\log_{10} p$ value compared with the other groups. Consistent with the conclusion of LEfSe and principal coordinates analysis that high F exposure and *L. johnsonii* BS15 affected colonic communities differently, we observed that the colon in mice present different microbial habitats with specific sets of microbes. Subsequently, we defined the OTUs that were chosen by both methods as control specific OTUs (hereafter: csOTUs), high F exposure sensitive OTUs (hereafter: fsOTUs, significantly changed compared with Ctrl group), as well as high F exposure and *L. johnsonii* BS15 co-sensitive OTUs (hereafter: flsOTUs, significantly changed compared with Ctrl group), respectively. In colon, we identified a total of 114 differential bacteria OTUs. As evaluation for an "effect value" of different treatments on microbial communities, we found 20, 86 and 18 bacteria for csOTUs, fsOTUs and flsOTUs, corresponding to an effect value of 5.9%, 21.1% and 13.4%, respectively (Fig. 5 C). Mean relative abundance of csOTUs, flOTUs, flsOTUs and their phyla level were showed by heatmap to observe how they're distributed in different groups (Fig. S4). To conclude, each experimental treatments supports a specialized subset of colonic bacteria, while the majority of the microbial communities are shared in three groups.

3.8. Identification of keystone OTUs and correlation between the keystone OTUs and renal- and TJ-related parameters

Next, we confirmed the extent to which high F exposure and *L. johnsonii* BS15 impacted microbial co-occurence patterns in colonic bacteria. For this, we constructed the co-occurrence network, identified network properties, and mapped the node of csOTUs, fsOTUs and flsOTUs for colonic bacterial community. As shown in Fig. 6 A, we tested for six modules contained relatively high proportions of differential species in the bacterial network. And we noted in the colonic network that differential species agglomerating according to different practical significance. The type of sensitivity of these module members to the specific practical significance (Fig. 6B) and their distribution in the bacterial co-occurrence network partially presented the drivers of bacteria dissimilarity shown in the result of CAP ordination. These models were consisted by different bacterial species (Fig. 6 C). The effect of high F exposure in the bacterial community was most apparent with three discrete modules (M2, M3 and M4), containing fsOTUs specific to high F induced variance. Additionally, these modules (M2, M3 and M4) were separated from three other modules (M1, M5 and M9) that primarily contained csOTUs and flsOTUs specific to the response patterns of No-treatment and probiotics-treament, respectively (Fig. 6D). Furthermore, we found the highly overlap of co-sensitive OTUs in the M2 comparing fsOTUs and flsOTUs. Finally, we identified keystone OTUs for the colonic network and visualized them by relative abundance and node degree (Fig. 6E). According to the results of Fig. 6E, we observed that partial fsOTUs and flsOTUs exhibited higher node degrees of co-occurrence than csOTUs. In bacterial communities, all OTUs were detected among low to high abundance along axis Y. The keystone OTUs were from the Bacteroidetes, such as *Bacteroidaceae* (OTU5, OTU794, OTU1035, and OTU48) and *Prevotellaceae*family (OTU18, OTU1005, OTU741, OTU651, OTU902, OTU170, OTU868, and OTU57) (Table S3). Subsequently, we observed that these keystone OTUs were correlated positively or negatively with renal clinical chemical parameters, peroxidation damage and antioxidant capacity as well as colonic permeability (Fig. 6F-H). The relative abundance of these keystone OTUs in were significantly higher in F group than that in Ctrl group, and the tendency was reversed in Prob group except OTU57 and OTU170.

In summary, we observe that high F exposure markedly influence colonic co-occurrence patterns of numerous bacteria, but supplementation with *L. johnsonii* BS15 effectively improve these negative influences. Additionally, these impacts altered, to a great extent, intestinal permeability and renal health largely independent of colonic bacterial abundance and their correlation relationships.

4. Discussion

The previous studies have revealed profound effects of drinking high F water by induced pathology of tissue and organs. As one of the most important metabolic and excretory organ to F, kidney is peculiarly prone to lesions under long-term high F exposure (Basha and Rao, 2014). In the previous studies on the changes of kidney in the state of fluorosis, most researches have reported altered cell signaling pathways, lipid peroxidation, autophagy and apoptosis (Luo et al., 2017a, 2017b). Our motivation was to demonstrate the mechainsm of the impact of drinking high F water by examining the alteration of gut microbiome. We also detected the preventive effect of priobiotic (*L. johnsonii* BS15). The maintenance of kidney health relies upon a delicate change among gut microbial communities, intestinal mucosa barrier and blood circulation system. Ritz (2011) proposed the concept of "Intestinal-renal syndrome", trying to illuminate the special association between gut and kidney. Intestinal inflammation and renal injury are inseparably linked as each causes and intensifies the other (Meijers and Evenepoel, 2011). Though various factors, such as oxidative stress, immune response and hypertension, can

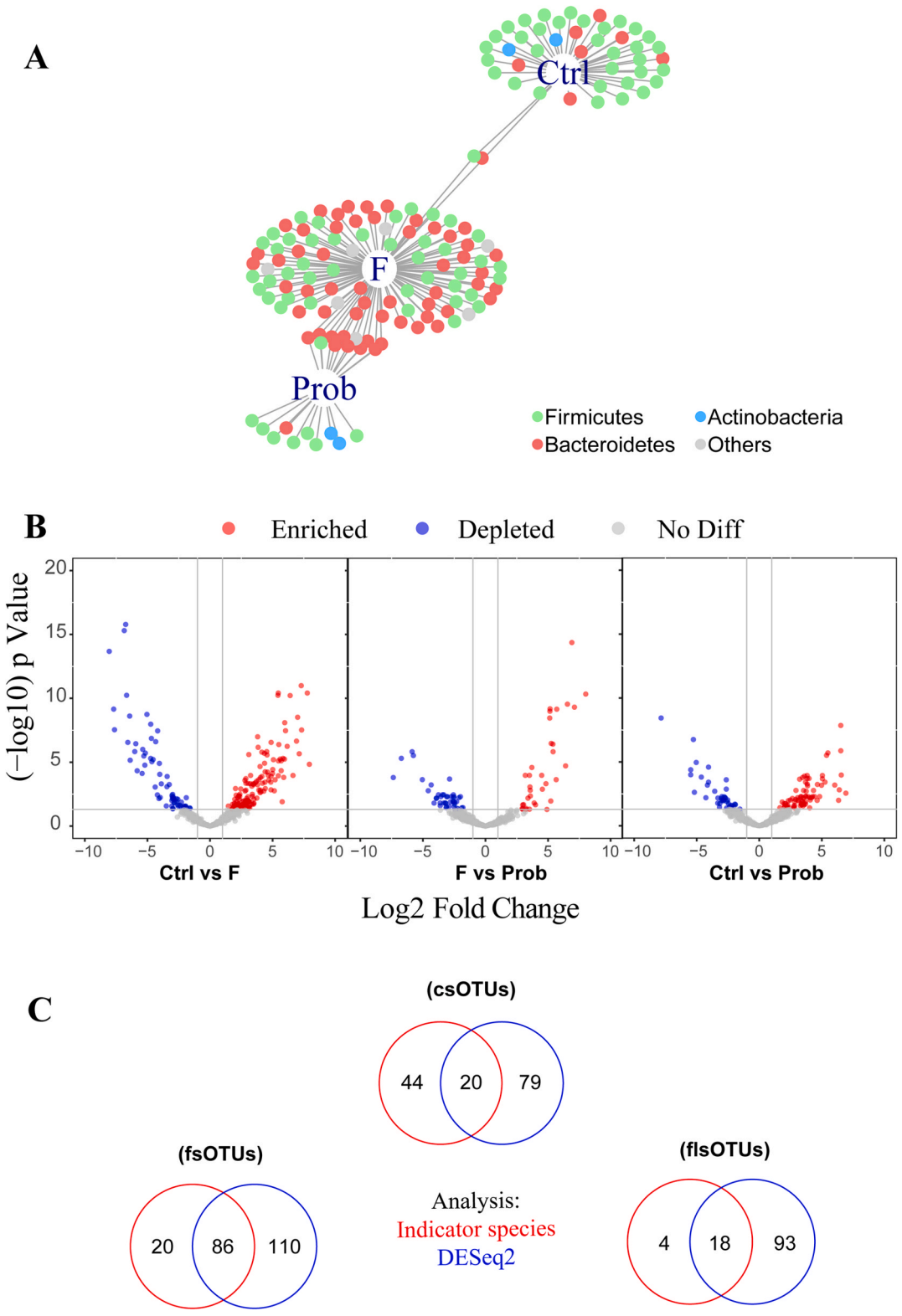

Fig. 5. Defining control specific and sensitive bacterial OTUs in colonic samples. (A) Bipartite networks of indicator species analysis. It display different treatment specific OTUs in the colonic bacterial communities using indicator species analysis. Circle represent individual bacteria and OTUs that are positively and significantly associated ($p < 0.05$) with one or more of different grouping factor (association(s) given by connecting lines). OTUs are colored according to their Phylum assignment. (B) Different treatments are enriched and depleted for certain OTUs. Enrichment and depletion of bacterial OTUs included in differential abundance analysis for each treatments compared with other treatments were determined using DESeq2 analysis. Each point represents an individual OTU, and the position along the x axis and y axis represents the abundance fold change and p value, respectively, compared with other group. (C) Venn diagrams show the number of OTUs responding to different grouping factor identified with indicator species analysis (red) and by DESeq2 analysis (blue). OTUs identified by both methods were defined as control specific OTUs (csOTUs), high F exposure sensitive OTUs (fsOTUs) as well as high F exposure and *L. johnsonii* BS15 co-sensitive OTUs (flsOTUs).

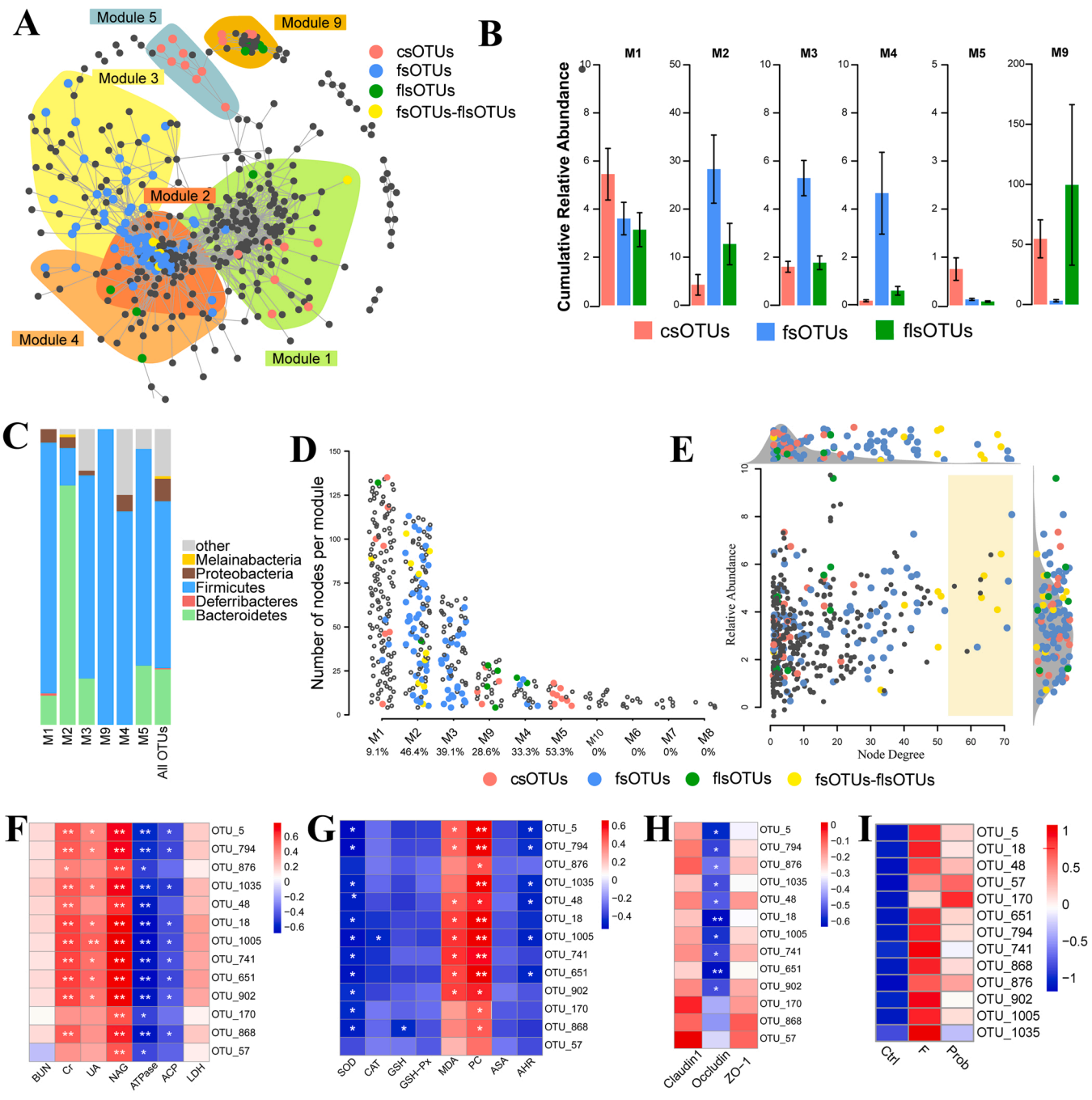

Fig. 6. Characteristics of co-occurrence networks and sensitive OTUs. (A) Co-occurrence networks visualizing significant correlations ($\rho > 0.6$, $P < 0.01$; indicated with gray lines) between OTU pairs in the Ctrl, F and Prob colonic bacterial communities. OTUs were colored by their association to the different representative meaning. Shaded areas represent the network modules containing csOTUs, flOTUs and flsOTUs. (B) Cumulative relative abundance of bacteria of different grouping sensitive modules in colonic network. The cumulative relative abundance in samples of csOTUs (red), flOTUs (blue) and flsOTUs (green) indicates the overall response of grouping sensitive modules to different treatments. (C) Qualitative taxonomic composition of grouping sensitive modules is reported as proportional OTUs numbers per phylum and compared to the overall taxonomic distribution in the entire dataset (column "all"). (D) Defining network modules. Plot showing the number of OTUs in the top 10 most populated modules for the colonic co-occurrence networks. OTUs were colored by their association to the different grouping factor. Percentages on the X-axis indicate the proportion of csOTUs, flOTUs and flsOTUs present in each module. (E) Degree of co-occurrence and abundance of csOTUs, flOTUs and flsOTUs. Relative abundance of all OTUs from the colonic microbial co-occurence network was plotted as a function of their degree of co-occurrence. OTUs were colored by their association to the different grouping and keystone OTUs (top 3% degree of co-occurrence) have yellow background. Side panels recapitulate the distributions of co-occurence degrees and abundance for the csOTUs, flOTUs and flsOTUs (circle colored by association to different treatments). Spearman's rank correlation between the keystone OTUs and (F) clinical biochemical parameters, (G) Oxidative stress and antioxidant damage, and (H) mRNA expression levels of colon tight junction proteins. (I) keystone OTUs that are significantly altered by excess fluoride intake compared with the control group and reverted by *L. johnsonii* BS15. The results were presented as heatmaps using R package *pheatmap*. Heatmap showed that partial microbial modules was intimately associated with renal and colonic functions, which was positively or negatively related to functional paramrter. Rho in the color key represented Spearman rank correlation coefficient. * $P < 0.05$ denoted statistical significance between the correlations of keystone OTUs and functional parameters.

affect the normal metabolism of the kidney, intestinal microbiota still plays an essential role as one of the main drivers (Andersen et al., 2017). Moreover, as the main organs for expelling toxins, kidney and colon are also closely related to each other in terms of integrity and functions. Hatch and Vaziri (1994) demonstrated that when renal metabolism declines, the colonic tissue replaces the kidney as the important site to get rid of toxins. Deficits in kidney function associated with colonic permeability exacerbate the accumulation of enterogenic toxin and other metabolic material in the blood and may eventually induce uraemia (Yang et al., 2018). Probiotic provides novel possibility to prevent and treat renal injury caused by long-term F exposure. However, a specific application of the presented treatment method requires further studies with greater grouping design, from multiple bowels, across different time points and accounting for the variation of metabolic material in the intestines, blood as well as damaged organs.

4.1. Differential changes in renal tissue and function of high F exposed and probiotic treated mice

In the present study, we first observed the histopathological lesions of kidney. The results showed that high F exposure could induce significant increase of the contents of Cr and UA as well as the activities of urinary NAG and renal LDH. The results of NAG activities are consistent with previous study by Xiong et al. (2007) which showed that high F exposure could increase the urine NAG activities of children. Supplementation with *L. johnsonii* BS15 significantly reduced the activities of urinary NAG and renal LDH as well as the contents of serum Cr and UA. Furthermore, high F exposure decreased the activities of Na^+/K^+-ATPase and ACP in kidney, while *L. johnsonii* BS15 significantly alleviated the reduction of these indexes, indicating that the application of probiotics could be effective to inhibit F-induced renal damages to structure and metabolic function. Recent studies have shown that renal structure is closely linked to its function (Xiong et al., 2007). Deficits in renal function were found in this study, suggesting that excessive F can result in morphological structure damages of kidney tubular and glomerular (Welling and Welling, 1988), whereas the kidney of the mice in Prob group only appears slight dilatation and congestion of capillaries between glomeruli and renal tubules. Additionally, there was a significant increase in the MDA and PC contents in the kidney of F group. Previous studies have reported that PC and MDA are the representative products of protein oxidation and lipid peroxidation, respectively (Kohen and Nyska, 2002). Therefore, our experimental results indicated that *L. johnsonii* BS15 effectively exerted beneficial effects against high F-induced lipid oxidative damages in the kidney. Meanwhile, ASA and AHR abilities, which can remove superoxide anion and hydroxyl racdical (Jiang et al., 2014), were significantly decreased by high F exposure in renal tissue. Nevertheless, a slight improvement of these total scavenging capabilities was detected by *L. johnsonii* BS15 in the kidney. In general, it is widely accepted that free radical balance between production and scavenging is dynamic and stable. In the present study, we measured antioxidant-associated enzymes (SOD, CAT, GSH-Px and GSH) to evaluate the effects of high F exposure and *L. johnsonii* BS15 on enzymatic and non-enzymatic antioxidant. As shown in the results, we found that high F exposure depleted these enzymes activities. With the exception of the slight change of CAT activity, *L. johnsonii* BS15 significantly improved the activities of the other three determined antioxidant enzymes in the renal tissue. SOD is considered as a main enzyme against superoxide radical, which can converts superoxide radical to hydrogen peroxide (Eraslan et al., 2007). And the significance of CAT in the organism is to breakdown hydrogen peroxide and reduce the potential toxicity of hydroxyl free radicals on tissues (Luo et al., 2012). Therefore, their functions are actually complementary to each other. According to the experimental results, we found F-induced accumulation of superoxide radicals and hydroxyl radicals in the kidney was protected by supplementation with *L. johnsonii* BS15. GSH is responsible to remove various reactive species by a non-enzymatic mechanism, whereas the alteration of the redox status of GSH (GSH-Px) could result in higher levels of oxidative stress and tissue injury (Kehrer and Klotz, 2015). Study by Eraslan et al. (2007) proved that CAT and GSH-Px scavenged excess of hydrogen peroxide and lipid peroxide under the influence of sodium fluoride together. Taken together, through these results in the present study, we found high F exposure can induce structural lesions and dysfunctions to the renal tissue by increasing the contents of MDA and PC, and reducing the capability in free radical-scavenging as well as the activities of antioxidant enzymes. However, supplementation with *L. johnsonii* BS15 can effectively protect the negative effects against high F exposure.

4.2. Differential responses of colon permeability, microbial composition and diversity

The toxicity of high F concentration on various tissues and organ has been reported and considered to be mediated by intestinal microbiota imbalance (Liu et al., 2019). Excessive F intake was reported to impair the intestinal development in rats (Wang et al., 2019), and the microbial structure in the intestines has been accepted to be closely related to the condition of intestinal development, which indicates the link between high F exposure and gut microbiota (Kåhrström et al., 2016). Previous work also showed that disruption or defects in intestinal barrier integrity could result in the instability of microorganism balance and other harmful substances may cross the epithelial barrier, leading to many intestinal and extraintestinal diseases (Kabat et al., 2014). In the present study, constant exposure of colonic tight junction proteins to excessive F reduced their levels of mRNA expression and decreases epithelial barrier function in mice. But beneficial changes caused by the supplementation with *L. johnsonii* BS15 on the mRNA expression of intestinal tight junction proteins in the colon were evaluated. Deficits in renal function induced by a leaky gut exacerbate the accumulation of endotoxins and bacterial products in the blood and may eventually cause diseases of various tissues and organs (Al Khodor and Shatat, 2017). Furthermore, the present study provided a characterization of the colonic microbiome of mice exposed to high F, involving the combination of more specific bacterial composition and deeper species association than previous F intake studies on modulating colonic microbiota environment. Detailed characterization of gut microbiota in relation to the renal injury induced by high F exposure has not been previously reported. In the present study, the different treatments of mice in Ctrl and F groups displayed distinct separations by compartment through the unconstrained PCoA ordinations analysis of bacteria. Similarly, such a differential distribution of colonic microbiota in Prob group was also found, although the separation is not obvious compared with the other two groups. To further conceptualize this, we also tested specific responses of bacteria to different treatments. This analysis method differs from unconstrained principal coordinate analysis in that technical factors can be controlled in the application process and it can be constrained to any interested factor to better comprehend the quantitative influence of the factor on the colonic microbial composition. Using this analysis to control individual difference, environment and technical factors (improper operation, biological replicate and sequencing batch), we found that in accordance with the PERMANOVA results, partial CAP-constrained by different treatment methods-highlighted both high F exposure and *L. johnsonii* BS15 effects on bacteria community. According to the result of CAP analysis, we observed significant effects of high F exposure and *L. johnsonii* BS15 on colonic microbial community, explaining approximately 25% of the total variation in bacteria. High F exposure was the most influential factor for the colonic bacteria, while *L. johnsonii* BS15 altered most of the variation induced by F. Additionally, we found the F group to be more diverse than the other two groups in colonic microbial communities, whereas *L. johnsonii* BS15 treatment affected species richness and diversity to small degree than community composition. This is consistent with previous research that observed species number and shannon index in the F group increased compared with control

group (Liu et al., 2019). Actually, variations in microbial community composition may not cause richness or diversity alteration because variations of some microbial taxa may be compensated by variation in others and single-variable measures of richness and diversity could mask relationships between individual relations and groups of microbial taxa (Hartmann and Widmer, 2006). Therefore, our results indicated that high F exposure and *L. johnsonii* BS15 affect colonic microbial communities differently.

The relative abundance of Firmicutes is increased in Prob samples compared with F samples, and the relative abundances of Bacteroidetes and Actinobacteria decrease from F samples to Prob samples, similar to previous study in which abundance of intestinal predominant flora influenced by *L. johnsonii* BS15 gradually restored to the control level (Sun et al., 2020). Metastats analysis was conducted to further observe differential abundant taxa between the three groups. As shown in the results, the mice exposed to high F showed significant alternation of the colon microbiome. *Bacteroides*, *Alloprevotella* and *Alistipes* were the most dominant bacterial genus in the colon in mice exposed to high F, and *Lactobacillus* was the most dominant bacterial genus from Prob group. By using LEfSe analysis, we also observed that the *L. johnsonii* BS15 serve an enrichment role for Firmicutes and *Lactobacillus* relative to high F exposed mice. The biomarkers enriched in the Prob group are simultaneously appeared in the colon microbes of Ctrl group compared with F group. The composition and diversity of gut microbial community are reported to be significantly affected by environmental condition (Chang et al., 2019). These results are same as the previous microbiome study, where Firmicutes, Bacteroidetes and *Lactobacillus* showed significant alteration in species difference analysis after high F exposure (Lin et al., 2019; Luo et al., 2016). Firmicutes is demonstrated to play an important role in the digestion of proteins and fat and can regulate the absorption of nutrients (Simpson and Campbell, 2015). Evidence supported that alteration of Firmicutes in the gut of mice might be associated with decreased weight induced by F exposure (Wang et al., 2017). Bacteroidetes is related to the metabolism of carbohydrate, bile acid and steroid, and promoting mucosal formation in the intestines (Li et al., 2017; Wu et al., 2018). *Lactobacillus* is involved in fibrinolytic, enzymatic and broad-spectrum antimicrobial activity, which can inhibit other bacterial growth especially harmful bacteria (Eom et al., 2015). Given that, *L. johnsonii* BS15 was considered as the first largest source of variation within the colon microbial communities of Prob samples under high F conditions. Next, we explored the changes of correlation between colonic microbial genus under different treatments. One of the striking alterations of the microbial taxa in Prob group shown in the correlation network was higher relevance of *Lactobacillus* with other genus, which has little or no strong correlation with other taxa in other two conditions (non-treatment and high F exposure). The connections between genera levels representing positive, significant correlation in the F group was clearly decreased comparing to that in the Ctrl group, but supplementation with *L. johnsonii* BS15 led to much stronger correlation among different bacterial genera levels, suggesting *L. johnsonii* BS15 enhanced the degree of correlation between difference species in the colon. Increasing lines of evidence showed that alternation in the intestinal microbial composition could be considered as a pathologic mediator in a variety of diseases (Sartor and Wu, 2017). As a common public hazard substance in the environment, excessive F has been demonstrated to be associated with gastrointestinal symptoms, such as intestinal damage and enteritis, which could be related to gut microbial community. Above mentioned results indicated that *L. johnsonii* BS15, as a probiotic strain, might be a effective preventive measure that modulate the colon microbiota to improve renal injury and its complications.

4.3. Effects of high F exposure and L. johnsonii BS15 treatment on keystone OTUs of colon microbiota

The concept of probiotics treatment postulates optimizing the composition and function of gut microbiota to maintain intestinal health and prevent the occurrence of visceral diseases. Its primary potential is targeted and specific interventions with intestinal microbial community. As a basis for implementing probiotics strategies into high F exposure mice, we demonstrated here to which extent and how the different processing conditions permit the manipulation of colonic microbiota. In the following study, we identified control specific OTUs (csOTUs), high F exposure sensitive OTUs (fsOTUs) as well as high F exposure and *L. johnsonii* BS15 co-sensitive OTUs (flsOTUs), respectively, in colonic microbial communities to explain the β-diversity patterns by different treatments. For example, the significant changes in bacterial abundance of sensitive bacteria OTUs under high F treatment were consistent with a separation by different factors in CAP analysis between F group and other groups.

In colonic co-occurrence network, 6 modules containing high proportions of control specific and sensitive OTUs were identified fsOTUs and flsOTUs responded to specific experimental condition (high F exposure and *L. johnsonii* BS15 treatments). Meanwhile, we found that keystone OTUs identified by relative abundance and node degree belong to module 2 and show negative effects on renal health and intestinal integrity. Among these keystone OTUs, OTU 5, OTU 794, OTU 1035, and OTU 868 were fsOTUs but not flsOTUs, suggesting that *L. johnsonii* BS15 reversed changes of these fsOTUs. We infer that reversed changes of OTU 5, OTU 794, OTU 1035 and OTU 868 in BS15-treated mice may be the underlying protected mechanism of *L. johnsonii* BS15 on kidney. Moreover, most of all fs-flsOTUs grouped were in module 2, which reflected that these sensitive species were consistently different from baseline under high F exposure or *L. johnsonii* BS15 treatment. And we infer that fs-flsOTUs and csOTUs were contributed to the unreconsitution of colon microbiota in *L. johnsonii BS15*-treated mice. Study by Mao et al. (2018) proved that the impaired barrier function is closely related to colonisation and composition of intestinal commensal bacteria. Effects of feeding condition on intestinal health were proved by directly modifying the integrity of intestinal mucosal and the structure of mucin or indirectly by regulating intestinal microbial compositions (Biasato et al., 2018; Llewellyn et al., 2018). In the co-occurrence network, we noted that the effects of high F exposure and *L. johnsonii* BS15 were mostly limited to non-keystone taxa in spite of significant influence of different grouping factor on β-diversity and network patterns. Partial fsOTUs exhibited high degrees of co-occurrence in the colonic network, revealing that high F intake could affect the highly co-occurring colonic species, which could belong to “core microbiome” members. Similarly, the flsOTUs, especially the species also sensitive to high F exposure separately, also included members with high degrees of co-occurrence. A subset of the most influential colonic community members (M2: fl-flsOTUs) may be widely manipulated with high F exposure, yet supplementation with *L. johnsonii* BS15 did not restored these high degree of co-occurrence species to control level. These phenomenon could possibly be one of the reasons why kidney biochemical indexes of Prob group did not completely restored to the level of Ctrl group, that is, *L. johnsonii* BS15 intake established a new structure and network of microbial community that different from the Ctrl and F groups. Keystone defined as a important taxa in the overall community that frequently associate with many other taxa (Ma et al., 2016). We finally identified 8 keystone OTUs to be high F exposure sensitive and 4 keystone OTUs to be *L. johnsonii* BS15 sensitive in the colonic bacteria. It is well known that most healthy adult and animal microbial communities in the intestines are dominated by only two phyla of bacteria, Gram-positive Firmicutes and Gram-negative Bacteroidetes, that together form the majority of the microbial structure of many individuals (Huttenhower et al., 2012). To date, Bacteroidetes, which predominantly metabolize protein, has been shown to be associated with the occurrence of chronic kidney disease (Jiang et al., 2017). And the colonization of Bacteroidetes is critical for inducing immune response in the intestinal tract, such as the balance between TH1 and TH2 responses (Ivanov et al., 2009). Through the subsequent results, it is obvious to find that high F exposure and *L. johnsonii* BS15 had profound

impacts on the species with high co-occurrence of Bacteroidetes in colon. In view of the above, we hypothesized that these keystones altered from Bacteroidetes might significantly affect the community of the entire colon network and alter the intergrity and permeability of the gut, thereby increasing the burden of renal metabolism in high F environment. The involvement of *L. johnsonii* BS15 could optimize the microbial structure by affecting the core and peripheral species in the colon, thus playing a certain protective role in the renal tissue under high F environment.

4.4. Strengths and limitations of this study

In this study, the preventive effect of BS15 on fluoride induced kidney injury was found, also indirectly suggesting that intestinal microbiota may be one of the key pathways and preventive methods of F induced renal injury. Meanwhile, through various analysis methods, four key OTUs involved in the regulation of BS15 on fluoride induced renal injury were detected, which provided theoretical support for the subsequent mechanism exploration. However, further studies are still needed to identify the exact strains from the identified four key OTUs that directly mediated F-induced renal damages. Since it remains very difficult to find out the key strain only based on 16 S rDNA sequencing, more methods (such as culture omics) should be applied in the subsequent studies to improve the possibility of eventurally finding this strain. (Weiss et al., 2016) Meanwhile, it is also important to further reveal the intermediate metabolite which connects the changes of intestinal microbiota and renal function.

5. Conclusion

These results demonstrated that supplementation with *L. johnsonii* BS15 could reverse high F induced renal oxidative damages through increasing the free-scavenging abilities and activities of antioxidant enzymes, which protects the kidney tissue from renal lesion and dysfunction. High F exposure and *L. johnsonii* BS15 treatment had marked effects on microbial structure and diversity in colon, and sensitive and well-connected species, which might be closely related to renal health under high F environment could be considered as key species among different treatments. The present study contributed to understand the link between colon microbiome and kidney health in high F environments and provided insights for applications of future probiotic therapy.

Funding

The present study was supported by Sichuan Science and Technology Program (2021YFH0097), Natural Science Foundation of Guangdong Province, China (Grant No: 2019A1515012115) and President Foundation of Nanfang Hospital, Southern Medical University (Grant No: 2020Z008). Both funding bodies provided funding support for the animal purchase and parameter determination.

CRediT authorship contribution statement

JX, HW, NS, DZ, YB, and XN: Conceptualization, Methodology. JX, NS, LL, XB, HH and HM: Project administration, Data curation, Writing-Original draft preparation. HW, BW, YW and DZ: Writing-Original draft preparation. HW, AC and SG: Writing-Reviewing and Editing JX and XN: upervision.All authors read and approved the final manuscript.

Ethical approval

All animal experiment procedures were conducted in accordance with the guidelines of the Animal Welfare Act and all procedures and protocols were approved by the Institutional Animal Care and Use Committee of the Sichuan Agricultural University (approval number: SYXKchuan2019–187).

Declaration of Competing Interest

The authors declare that they have no known competing financial interests or personal relationships that could have appeared to influence the work reported in this paper.

Availability of Data and Materials

16S rRNA sequencing reads have uploaded to NCBI. The accession code of sequence reads Archive in the National Center for Biotechnology Information (NCBI) BioProject database: PRJNA693263.

Supplementary data to this article can be found at Supplementary files 1 and 2.

Acknowledgements

The authors gratefully acknowledge the help from Mr. Yao Zhipeng and Mr. Wan Zhiqiang for all the hard working during the data analysis. Also, we really appreciate the supports provided by the undergraduates during the animal feeding and sampling.

Appendix A. Supporting information

Supplementary data associated with this article can be found in the online version at doi:10.1016/j.ecoenv.2021.113006.

References

Al Khodor, S., Shatat, I.F., 2017. Gut microbiome and kidney disease: a bidirectional relationship. Pedia Nephrol. 32 (6), 921–931. https://doi.org/10.1007/s00467-016-3392-7.

Andersen, K., Kesper, M.S., Marschner, J.A., Konrad, L., Ryu, M., Kumar Vr, S., Kulkarni, O.P., Mulay, S.R., Romoli, S., Demleitner, J., Schiller, P., Dietrich, A., Müller, S., Gross, O., Ruscheweyh, H.J., Huson, D.H., Stecher, B., Anders, H., 2017. Intestinal dysbiosis, barrier dysfunction, and bacterial translocation account for ckd-related systemic inflammation. J. Am. Soc. Nephrol. 28 (1), 76–83. https://doi.org/10.1681/ASN.2015111285.

Ayoob, S., Gupta, A.K., 2006. Fluoride in drinking water: a review on the status and stress effects. Crit. Rev. Environ. Sci. Technol. 36 (6), 433–487. https://doi.org/10.1080/10643380600678112.

Basha, S.K., Rao, K.J., 2014. Sodium fluorine induced histopathalogical changes in liver and kidney of albino mice. Acta Chim. Pharm. Indica 4 (1), 58–62.

Biasato, I., Ferrocino, I., Biasibetti, E., Grego, E., Dabbou, S., Sereno, A., Gai, F., Gasco, F., Schiavone, A., Cocolin, L., Capucchio, M.T., 2018. Modulation of intestinal microbiota, morphology and mucin composition by dietary insect meal inclusion in free-range chickens. BMC Vet. Res 14 (1), 383. https://doi.org/10.1186/s12917-018-1690-y.

Caporaso, J.G., Kuczynski, J., Stombaugh, J., Bittinger, K., Bushman, F.D., Costello, E.K., Fierer, N., Peña, A.G., Goodrich, J.K., Gordon, J.I., Huttley, G.A., Kelley, S.T., Knights, D., Koenig, J.E., Ley, R.E., Lozupone, C.A., McDonald, D., Muegge, B.D., Pirrung, M., Reeder, J., Sevinsky, J.R., Turnbaugh, P.J., Walters, W.A., Widmann, J., Yatsunenko, T., Zaneveld, J., Knight, R., 2021. QIIME allows analysis of high-throughput community sequencing data. Nat. Methods. 7 (5), 335–336. https://doi.org/10.1038/nmeth.f.303.

Chang, X., Li, H., Feng, J., Chen, Y., Nie, G., Zhang, J., 2019. Effects of cadmium exposure on the composition and diversity of the intestinal microbial community of common carp (Cyprinus carpio L.). Ecotoxicol. Environ. Saf. 171, 92–98. https://doi.org/10.1016/j.ecoenv.2018.12.066.

Eom, J.S., Song, J., Choi, H.S., 2015. Protective effects of a novel probiotic strain of *Lactobacillus plantarum* jsa22 from traditional fermented soybean food against infection by Salmonella enterica serovar typhimurium. J. Microbiol Biotechnol. 25 (4), 479–491. https://doi.org/10.4014/jmb.1501.01006.

Eraslan, G., Kanbur, M., Silici, S., 2007. Evaluation of propolis effects on some biochemical parameters in rats treated with sodium fluoride. Pestic. Biochem. Physiol. 88 (3), 273–283. https://doi.org/10.1016/j.pestbp.2007.01.002.

Hartman, K., van der Heijden, M.G.A., Wittwer, R.A., Banerjee, S., Walser, J.C., Schlaeppi, K., 2018. Correction to: Cropping practices manipulate abundance patterns of root and soil microbiome members paving the way to smart farming. Microbiome 6 (1), 14. https://doi.org/10.1186/s40168-017-0389-9.

Hartmann, M., Widmer, F., 2006. Community structure analyses are more sensitive to differences in soil bacterial communities than anonymous diversity indices. Appl. Environ. Microbiol 72 (12), 7804–7812. https://doi.org/10.1128/AEM.01464-06.

Hatch, M., Vaziri, N.D., 1994. Enhanced enteric excretion of urate in rats with chronic renal failure. Clin. Sci. (Lond.) 86 (5), 511–516. https://doi.org/10.1042/cs0860511.

Hida, M., Aiba, Y., Sawamura, S., Koga, Y., 1996. Inhibition of the accumulation of uremic toxins in the blood and their precursors in the feces after oral administration of Lebenin, a lactic acid bacteria preparation, to uremic patients undergoing hemodialysis. Nephron 74 (2), 349–355. https://doi.org/10.1159/000189334.

Huttenhower, C., Gevers, D., Knight, R., et al., 2012. The human microbiome project (hmp) consortium. structure, function and diversity of the healthy human microbiome. Nature 486 (7402), 207–214. https://doi.org/10.1038/nature11234.

Ivanov, I.I., Atarashi, K., Manel, N., Brodie, E.L., Shima, T., Karaoz, U., Wei, D., Goldfarb, K.C., Santee, C.A., Lynch, S.V., Tanoue, T., Imaoka, A., Itoh, K., Takeda, K., Umesaki, Y., Honda, K., Littman, D.R., 2009. Induction of intestinal Th17 cells by segmented filamentous bacteria. Cell 139 (3), 485–498. https://doi.org/10.1016/j.cell.2009.09.033.

Jiang, S., Xie, S., Lv, D., Wang, P., He, H., Zhang, T., Zhou, Y., Lin, Q., Zhou, H., Jiang, J., Nie, J., Hou, F., Chen, Y., 2017. Alteration of the gut microbiota in Chinese population with chronic kidney disease. Sci. Rep. 7 (1), 2870. https://doi.org/10.1038/s41598-017-02989-2.

Jiang, W.D., Liu, Y., Hu, K., 2014. Copper exposure induces oxidative injury, disturbs the antioxidant system and changes the Nrf2/ARE (CuZnSOD) signaling in the fish brain: protective effects of myo-inositol. Aquat. Toxicol. 155, 301–313. https://doi.org/10.1016/j.aquatox.2014.07.003.

Kabat, A.M., Srinivasan, N., Maloy, K.J., 2014. Modulation of immune development and function by intestinal microbiota. Trends Immunol. 35 (11), 507–517. https://doi.org/10.1016/j.it.2014.07.010.

Kåhrström, C.T., Pariente, N., Weiss, U., 2016. Intestinal microbiota in health and disease. Nature 535 (7610), 47. https://doi.org/10.1038/535047a.

Kehrer, J.P., Klotz, L.O., 2015. Free radicals and related reactive species as mediators of tissue injury and disease: implications for Health. Crit. Rev. Toxicol. 45 (9), 765–798. https://doi.org/10.3109/10408444.2015.1074159.

Kohen, R., Nyska, A., 2002. Oxidation of biological systems: oxidative stress phenomena, antioxidants, redox reactions, and methods for their quantification. Toxicol. Pathol. 30 (6), 620–650. https://doi.org/10.1080/01926230290166724.

Li, M., Shang, Q., Li, G., Wang, X., Yu, G., 2017. Degradation of marine algae-derived carbohydrates by bacteroidetes isolated from human gut microbiota. Mar. Drugs 15 (4), 92. https://doi.org/10.3390/md15040092.

Liu, J., Wang, H.W., Lin, L., Miao, C., Zhang, Y., Zhou, B., 2019. Intestinal barrier damage involved in intestinal microflora changes in fluoride-induced mice. Chemosphere 234, 409–418. https://doi.org/10.1016/j.chemosphere.2019.06.080.

Llewellyn, S.R., Britton, G.J., Contijoch, E.J., Vennaro, O.H., Mortha, A., Colombel, J.F., Grinspan, A., Clemente, J.C., Merad, M., Faith, J.J., 2018. Interactions between diet and the intestinal microbiota alter intestinal permeability and colitis severity in mice. e2 Gastroenterology 154 (4), 1037–1046. https://doi.org/10.1053/j.gastro.2017.11.030.

Luo, Q., Cui, H., Deng, H., Kuang, P., Liu, H., Lu, Y., Fang, J., Zuo, Z., Deng, J., Li, Y., Wang, X., Zhao, L., 2017a. Histopathological findings of renal tissue induced by oxidative stress due to different concentrations of fluoride. Oncotarget 8 (31), 50430–50446. https://doi.org/10.18632/oncotarget.17365.

Luo, Q., Cui, H., Deng, H., Kuang, P., Liu, H., Lu, Y., Fang, J., Zuo, Z., Deng, J., Li, Y., Wang, X., Zhao, L., 2017b. Sodium fluoride induces renal inflammatory responses by activating NF-κB signaling pathway and reducing anti-inflammatory cytokine expression in mice. Oncotarget 8 (46), 80192–80207. https://doi.org/10.18632/oncotarget.

Luo, Q., Cui, H., Peng, X., et al., 2012. Intestinal oxidative stress in broilers caused by high dietary fluorine. Fluoride 45 (4), 349–356. https://doi.org/10.1186/2050-6511-13-9.

Luo, Q., Cui, H., Peng, X., Fang, J., Zuo, Z., Deng, J., Liu, J., Deng, Y., 2016. Dietary high fluorine alters intestinal microbiota in broiler chickens. Biol. Trace Elem. Res 173 (2), 483–491. https://doi.org/10.1007/s12011-016-0672-9.

Ma, B., Wang, H., Dsouza, M., Lou, J., He, Y., Dai, Z., Brookes, P.C., Xu, J., Gilbert, J.A., 2016. Geographic patterns of co-occurrence network topological features for soil microbiota at continental scale in eastern China. ISME J. 10 (8), 1891–1901. https://doi.org/10.1038/ismej.2015.261.

Malin, A.J., Lesseur, C., Busgang, S.A., Curtin, P., Wright, R.O., Sanders, A.P., 2019. Fluoride exposure and kidney and liver function among adolescents in the United States: NHANES, 2013-2016. Environ. Int. 132, 105012 https://doi.org/10.1016/j.envint.2019.105012.

Mao, K., Baptista, A.P., Tamoutounour, S., Zhuang, L., Bouladoux, N., Martins, A.J., Huang, Y., Gerner, M.Y., Belkaid, Y., Germain, R.N., 2018. Innate and adaptive lymphocytes sequentially shape the gut microbiota and lipid metabolism. Nature 554 (7691), 255–259. https://doi.org/10.1038/nature25437.

Meijers, B.K., Evenepoel, P., 2011. The gut-kidney axis: indoxyl sulfate, p-cresyl sulfate and CKD progression. Nephrol. Dial. Transpl. 26 (3), 759–761. https://doi.org/10.1093/ndt/gfq818.

Petersson, L.G., Magnusson, K., Hakestam, U., Baigi, A., Twetman, S., 2011. Reversal of primary root caries lesions after daily intake of milk supplemented with fluoride and probiotic lactobacilli in older adults. Acta Odontol. Scand. 69 (6), 321–327. https://doi.org/10.3109/00016357.2011.568962.

Ritz, E., 2011. Intestinal-renal syndrome: mirage or reality? Blood Purif. 31 (1–3), 70–76. https://doi.org/10.1159/000321848.

Sartor, R.B., Wu, G.D., 2017. Roles for intestinal bacteria, viruses, and fungi in pathogenesis of inflammatory bowel diseases and therapeutic approaches. e4 Gastroenterology 152 (2), 327–339. https://doi.org/10.1053/j.gastro.2016.10.012.

Simpson, H.L., Campbell, B.J., 2015. Review article: dietary fibre-microbiota interactions. Aliment Pharm. Ther. 42 (2), 158–179. https://doi.org/10.1111/apt.13248.

Sun, N., Ni, X., Wang, H., Xin, J., Zhao, Y., Pan, K., Jing, B., Zeng, D., 2020. Probiotic *Lactobacillus johnsonii* BS15 prevents memory dysfunction induced by chronic high-fluorine intake through modulating intestinal environment and improving gut development. Probiotics Antimicrob. Proteins 12 (4), 1420–1438. https://doi.org/10.1007/s12602-020-09644-9.

Vaziri, N.D., Liu, S.M., Lau, W.L., Khazaeli, M., Nazertehrani, S., Farzaneh, S.H., Kieffer, D.A., Adams, S.H., Martin, R.J., 2014. High amylose resistant starch diet ameliorates oxidative stress, inflammation, and progression of chronic kidney disease. PLoS One 9 (12), e114881. https://doi.org/10.1371/journal.pone.0114881.

Wang, H.W., Liu, J., Zhao, W.P., Zhang, Z., Li, S., Li, S., Zhu, S., Zhou, B., 2019. Effect of fluoride on small intestine morphology and serum cytokine contents in rats. Biol. Trace Elem. Res 189 (2), 511–518. https://doi.org/10.1007/s12011-018-1503-y.

Wang, H.W., Zhao, W.P., Tan, P.P., Liu, J., Zhao, J., Zhou, B., 2017. The MMP-9/TIMP-1 system is involved in fluoride-induced reproductive dysfunctions in female mice. Biol. Trace Elem. Res 178 (2), 253–260. https://doi.org/10.1007/s12011-016-0929-3.

Weiss, S., Van Treuren, W., Lozupone, C., Faust, K., Friedman, J., Deng, Y., Xia, L.C., Xu, Z.Z., Ursell, L., Alm, E.J., Birmingham, A., Cram, J.A., Fuhrman, J.A., Raes, J., Sun, F., Zhou, J., Knight, R., 2016. Correlation detection strategies in microbial data sets vary widely in sensitivity and precision. ISME J. 10 (7), 1669–1681. https://doi.org/10.1038/ismej.2015.235.

Welling, L.W., Welling, D.J., 1988. Relationship between structure and function in renal proximal tubule. J. Electron Microsc. Tech. 9 (2), 171–185. https://doi.org/10.1002/jemt.1060090205.

Wu, S., Luo, T., Wang, S., Zhou, J., Ni, Y., Fu, Z., Jin, Y., 2018. Chronic exposure to fungicide propamocarb induces bile acid metabolic disorder and increases trimethylamine in C57BL/6J mice. Sci. Total Environ. 642, 341–348. https://doi.org/10.1016/j.scitotenv.2018.06.084.

Xin, J., Zeng, D., Wang, H., Ni, X., Yi, D., Jing, B., 2014. Preventing non-alcoholic fatty liver disease through *Lactobacillus johnsonii* BS15 by attenuating inflammation and mitochondrial injury and improving gut environment in obese mice. Appl. Microbiol Biotechnol. 98 (15), 6817–6829. https://doi.org/10.1007/s00253-014-5752-1.

Xin, J., Wang, H., Sun, N., Bughio, S., Zeng, D., Li, L., Wang, Y., Khalique, A., Zeng, Y., Pan, K., Jing, B., Ma, H., Bai, Y., Ni, X., 2021. Probiotic alleviate fluoride-induced memory impairment by reconstructing gut microbiota in mice. Ecotoxicol. Environ. Saf. 215, 112108 https://doi.org/10.1016/j.ecoenv.2021.112108.

Xiong, X., Liu, J., He, W., Xia, T., He, P., Chen, X., Yang, K., Wang, A., 2007. Dose-effect relationship between drinking water fluoride levels and damage to liver and kidney functions in children. Environ. Res 103 (1), 112–116. https://doi.org/10.1016/j.envres.2006.05.008.

Yang, T., Richards, E.M., Pepine, C.J., Raizada, M.K., 2018. The gut microbiota and the brain-gut-kidney axis in hypertension and chronic kidney disease. Nat. Rev. Nephrol. 14 (7), 442–456. https://doi.org/10.1038/s41581-018-0018-2.